NUMERICAL AND EXPERIMENTAL ANALYSIS OF A REPRESENTATIVE ADF HELICOPTER FUSELAGE

Dylan Brunello*, Gareth Clarke, Rami Reddy*
***Defence Science Technology Organisation**
Dylan.Brunello@dsto.defence.gov.au

Keywords: *helicopter fuselage, CFD, aerodynamics, wind tunnel*

Abstract

This paper presents the findings of an investigation into the aerodynamic characteristics of a representative Australian Defence Force (ADF) helicopter fuselage. Numerical and experimental methods were used to develop a database of aerodynamic coefficients suitable for flight dynamic and slung load modelling. A combined experimental and numerical approach was used for the analysis. To provide a set of experimental data, a 1:10 scale model representative of an ADF helicopter fuselage was tested in the Defence Science Technology Organisation (DSTO) Low Speed Wind Tunnel (LSWT). Two Computational Fluid Dynamics (CFD) solvers were used to estimate the aerodynamic forces and moments on a helicopter fuselage geometry for a range of flow conditions. Calculated results compare reasonably well with measured data for lower onset flow angles. The inclusion of the wind tunnel support in the numerical model was shown to improve the correlation between the experimental and numerical results.

1 Introduction

Helicopter flight dynamic and slung load models are required for research in support of Australian Defence Force (ADF) operations. Research activities include operations analysis, human in-the-loop simulations and accident investigations. The development of 'high fidelity' simulation models requires a comprehensive database of dynamic and aerodynamic characteristics for each individual aircraft component.

Fuselage aerodynamic characteristics directly affect helicopter flight dynamic and slung load simulations. During the development of new aircraft, information relating to these characteristics is collected by the manufacturer. This information is often not available to third parties. As a consequence, DSTO has sought alternative means of acquiring specific data to improve the fidelity of ADF helicopter simulation models.

A number of studies have been conducted that estimate the aerodynamic characteristics of helicopter fuselage geometries. These studies often focus on the lift and drag contribution of the fuselage in a forward flight condition [1, 2]. Another common research area is the interaction between the fuselage and the main and tail rotors [3]. An emphasis is placed on the development of numerical methods with experimental data used to validate the findings. Studies of this nature are useful for the analysis of new and existing aircraft configurations. However, they focus on a limited range of flight conditions making them less suitable for flight modelling purposes.

The focus of this study is the development of a fuselage aerodynamic coefficient database suitable for the helicopter modelling at DSTO. Currently research at DSTO utilises helicopter flight dynamic modes and a simulation model of a helicopter fuselage being transported as a slung load beneath a Chinook CH-47D helicopter. These models require fuselage aerodynamic coefficient data that span $\pm 180^{o}$ for pitch and yaw. Data is required for the fuselage in isolation - the effect of the rotor system is separately modelled within the flight dynamic simulation. The slung load model assumes the rotors are removed for transport.

A preliminary numerical investigation was conducted using the commercial CFD solver *ANSYS Fluent*. Following this, results from the preliminary simulations were used to guide the design of a helicopter fuselage wind tunnel model and support system. The model was tested in the DSTO LSWT where aerodynamic force and moment data was collected for a range of flow angles and fuselage configurations.

A second numerical investigation was conducted using the open source CFD solver *OpenFOAM*. Predictions from *OpenFOAM* and *Fluent* were compared to establish a level of confidence in *OpenFOAM*. Following this, the influence of the wind tunnel supports was assessed using CFD simulations.

2 Experimental Method

2.1 Wind Tunnel Model

A 1:10 scale model representative of an ADF helicopter was built for testing in the DSTO LSWT. The geometry was based on an openly available Computer Aided Design (CAD) file.

The model comprises of a fuselage, stub wings and tail surfaces. To streamline the fuselage and reduce interactional aerodynamic effects some of the smaller and more complicated features of the CAD model were removed or simplified. This included the landing gears and other smaller features such as aerials.

The model is made from a combination of polyurethane and aluminium components supported by a steel frame. An internal strain gauge balance was used to measure the aerodynamic loads on the model.

To meet the data requirements of both flight dynamic and slung load modelling two different mounting points are available, one through the rotor hub and the other through the starboard stub wing. To allow for pitch and yaw combinations to be tested a pivot mechanism was incorporated into the pylon support. The manually adjusted pivot mechanism can be cycled through two degree increments from 22^{o} to -8^{o} yaw or pitch when using the rotor hub or stub wing mounts respectively. This, together with the $\pm 180^{o}$ of rotation provided by the wind tunnel underfloor turntable, provides the range of angle combination required by the DSTO simulation models.

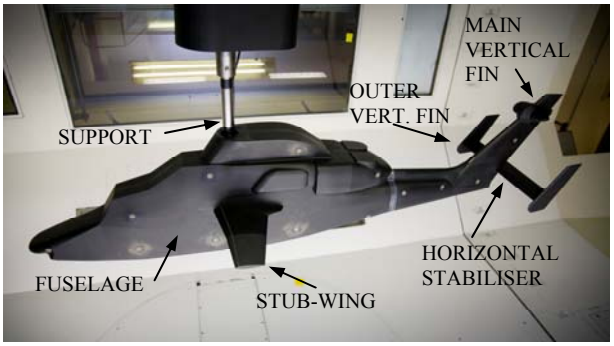

Fig. 1. Wind tunnel model

2.2 Test Facility

The DSTO Low Speed Wind Tunnel (LSWT) is a conventional, single return, closed circuit wind tunnel with a contraction ratio of 4:1. The test section has an irregular octagonal cross section that measures 9 *ft* wide by 7 *ft* tall. The tunnel is capable of airspeeds up to 100 *m/s* with the free stream turbulence generally below 0.7 %.

2.3 Test Program

Fuselage force and moment data has been obtained for a range of pitch and yaw configurations. Testing was conducted at a speed of 50 *m/s*. Transition strips were used to minimise Reynolds number effects and to create a turbulent boundary layer over the model. In addition to the force and moment data collected, flow visualisation was conducted using wool tufts and smoke to characterise some of the general flow phenomena.

3 Numerical Method

This section details the numerical studies that were carried out using the two CFD solvers *ANSYS Fluent* and *OpenFOAM*.

3.1 Preliminary Investigation

The commercial CFD software *ANSYS Fluent* was used to conduct a preliminary numerical investigation prior to the wind tunnel test program. The aim was to

- develop an initial data set to update existing flight dynamic and slung load models
- provide information required to select a suitable load balance and to design the wind tunnel model and its supports

3.1.1 Grid

The fuselage geometry used in the simulations was based on the CAD file used to develop the wind tunnel model. A simplified rotor hub was added and the CAD surfaces were 'cleaned up' to create a watertight geometry suitable for CFD modelling.

A hybrid unstructured grid was created using the grid generation software *ANSYS GAMBIT*. Triangular prism cells were extruded from the surface of the model to better resolve the boundary layer. Tetrahedral cells were used to populate the remainder of the spherical domain. The sensitivity of the solution to the domain boundary and the grid density was evaluated. A domain radius of 15 fuselage lengths (~220 *m*) and a cell count of 9×10^6 were adequate to provide a near grid independent solution.

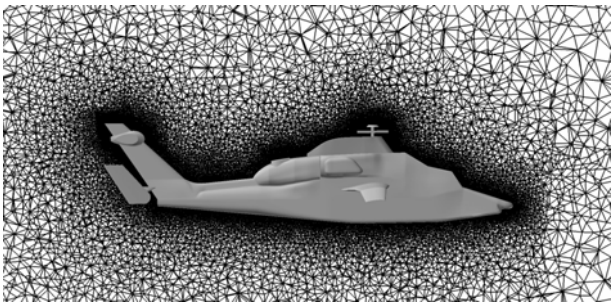

Fig. 2. CFD grid used in preliminary investigation

3.1.2 ANSYS Fluent Flow Solver

Steady state simulations were performed for a range of pitch and yaw angles. The incompressible Reynolds Averaged Navier-Stokes (RANS) equations were solved using the *Fluent* pressure based segregated solver. Pressure velocity coupling was treated using the SIMPLE (Semi Implicit Method for Pressure Linked Equations) algorithm [4]. The Menter *kω-SST* turbulence model was used to close the RANS equations [5]. Previous studies have suggested that this is a suitable model for flow about a helicopter fuselage [6]. Second order schemes were used to minimise the numerical diffusion.

3.1.3 Simulation Setup

To match the conditions of a helicopter fuselage being transported as a slung load, a velocity of 41 *m*/s (~80 *knots*) was prescribed for the domain inlet. Turbulence intensity at the inlet was set to 0.5 % to approximate free air. The *Fluent* Enhanced Wall Treatment (EWT) was used at the model surface. The EWT switches between a low Reynolds formulation and an empirical 'law of the wall' treatment depending on the non-dimensional wall spacing, y^+. The initial spacing at the wall was sufficiently small such that a low Reynolds formulation was used for the entire surface. Onset flow angles were created by rotating the domain boundaries and the inlet velocity vector relative to the fuselage.

3.2 Subsequent Investigation

A second numerical investigation was conducted using the open source CFD software *OpenFOAM* (version 2.0.x). The aim of the investigation was to

- assess the capability of *OpenFOAM* by comparing simulation results against *Fluent* results for the same test case
- account for the interference caused by the wind tunnel supports

3.2.1 Grid

Two sets of grids were used for the simulations detailed in this section: one for the comparison between *OpenFOAM* and *Fluent*, the other for the support interference investigation.

For simplicity, the comparisons between *OpenFOAM* and *Fluent* used a similar grid to the preliminary investigation. The main difference between the grid structures was the initial spacing at the wall. The wall spacing was

increased to allow for standard 'law of the wall' functions to be applied at the model surface. This reduced the number of elements in the grid and the computational cost of the simulations.

The scaled down CAD geometry used for the wind tunnel model was the basis of the interference investigation. To account for the influence of the wind tunnel supports additional geometry was added to a number of simulations. The grid generation software *Pointwise* was used to create an unstructured tetrahedral domain. The fully unstructured approach simplified the re-meshing required for each flow onset angle. To better control the grid density and more accurately resolve the flow about the model the domain was split into several regions. A rectangular box domain was used to align the flow with the domain boundaries.

The sensitivity of the solution to the grid density and the domain spacing was assessed. A minimum far field spacing of 20 fuselage lengths and a cell count of 6×10^6 provided adequate grid independence for the interference investigation.

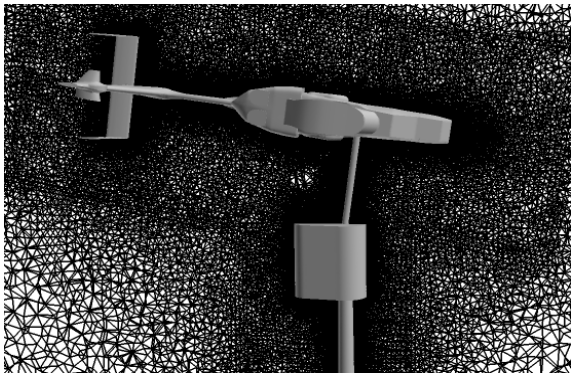

Fig. 3. CFD grid used to assess side support interference

3.2.2 *OpenFOAM Flow Solver*

The steady state incompressible RANS solver, *simpleFOAM*, was used for the *OpenFOAM* simulations. The segregated solver uses the SIMPLE algorithm to treat the pressure-velocity coupling. To maintain consistency with the *Fluent* simulations, the Menter *kω-SST* turbulence model was used. Second order schemes were used for most terms. However, first order schemes were required to maintain stability for the turbulent kinetic energy (k) and specific turbulent dissipation (ω).

3.2.3 *Simulation Setup*

The flow conditions used in the solver comparison were the same as the conditions in the preliminary investigation. Similar *OpenFOAM* and *Fluent* boundary conditions were applied where possible. *OpenFOAM* is not equipped with a wall treatment equivalent to the *Fluent* EWT. To keep the simulations consistent, both solvers used standard 'law of the wall' functions at the fuselage surface. The average y^+ value for the *Fluent* and *OpenFOAM* simulations was approximately 50, within the required range.

The support interference simulations were set up to replicate the conditions in the wind tunnel where possible. At the domain inlet a fixed velocity was specified to give a similar Reynolds number to that of the wind tunnel tests. Turbulence intensity at the inlet was set to 0.7 % to match the measured conditions in the wind tunnel.

4 Results

Three sets of results are presented in this section. Comparisons are made between the preliminary CFD data set generated in *Fluent* and the data from the LSWT. Following this, *OpenFOAM* and *Fluent* simulations are compared using a benchmark case to assess the performance of *OpenFOAM* compared to *Fluent*. Finally, results are shown for *OpenFOAM* simulations that aim to account for the interference caused by the wind tunnel supports. The axes system used in the results section is shown in Figure 4.

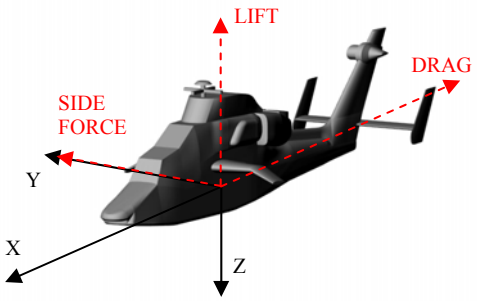

Fig. 4. Body axes (black) and wind axes (red)

4.1 Preliminary CFD and Wind Tunnel Comparison

This section compares results from the preliminary CFD investigation with wind tunnel data. Results are presented in conventional helicopter body axes, Figure 4. Data is shown over two separate yaw ranges for clarity. The intention of this comparison is to assess the general trends of the two data sets and to highlight some of the distinct flow features.

4.1.1 Aerodynamic Coefficients

The variation of force coefficients with yaw angle is shown in Figures 5 and 6. The simulated force coefficients generally compare well with the experimental data, particularly for yaw angles between ±45°. Within this range, the variation of the Y force coefficient (C_Y) is approximately linear. The magnitude of C_Y predicted in *Fluent* is approximately 15 % lower than the wind tunnel data. The force coefficient in the Z direction (C_Z) compares very well, particularly for yaw angles from 0° to 45°; between 0° and -45° the numerical results under predict the experimental data. The X force coefficient (C_X) is mostly over predicted which can be partially attributed to an increase in drag caused by the inclusion of a simplified rotor hub in the numerical model. It is also typical for CFD methods to over predict the drag values at low onset flow angles [3, 6]. Beyond ±45° yaw there is a significant divergence of the Y and Z force coefficients. The wind tunnel data shows the Y force coefficient to be almost sinusoidal. The numerical results remain relatively constant, between ±45° and ±135°, significantly under predicting the experimental data. For the Z force coefficient the numerical results fail to capture variation observed in the experimental data in particular the dip at ±90°. Further research is required to better understand the reason for the discrepancies.

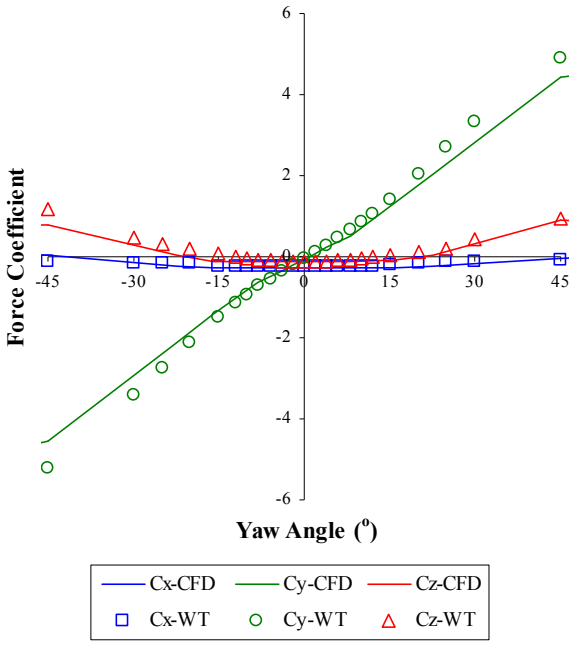

Fig. 5. Force coefficients in the X, Y and Z directions against yaw angle (yaw range ±45°)

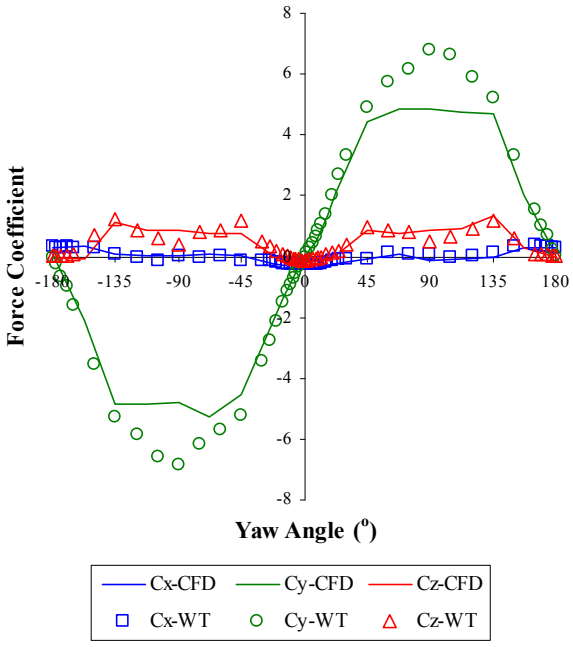

Fig. 6. Force coefficients in the X, Y and Z directions against yaw angle (yaw range ±180°)

Figure 7 shows the variation of moment coefficients for the yaw range ±45°. General agreement can be seen in the trends of the two data sets. The moment coefficient about the Z axis (M_Z) shows good agreement at 0° yaw; M_Z is positive at 0° yaw due to the asymmetric alignment of the outer vertical fins. The positive moment helps to offset the main rotor torque

during forward flight. In the case of a fuselage being transported as a slung load, this may have implications on the stability of the load. The moments about the *Z* axis are influenced by the 'local' flow yaw angle at the vertical tail surfaces. Small differences in the flow alignment through the tail can significantly impact the moment contribution from the tail. The change in local flow direction is illustrated in Figure 10.

The moment coefficient about the *Y* axis at 0° yaw is over predicted by the numerical simulations. The drag created by the simplified rotor hub contributes to the over prediction. The overall agreement between the results is fairly poor. Again, further research is required to determine the cause(s) of the discrepancies.

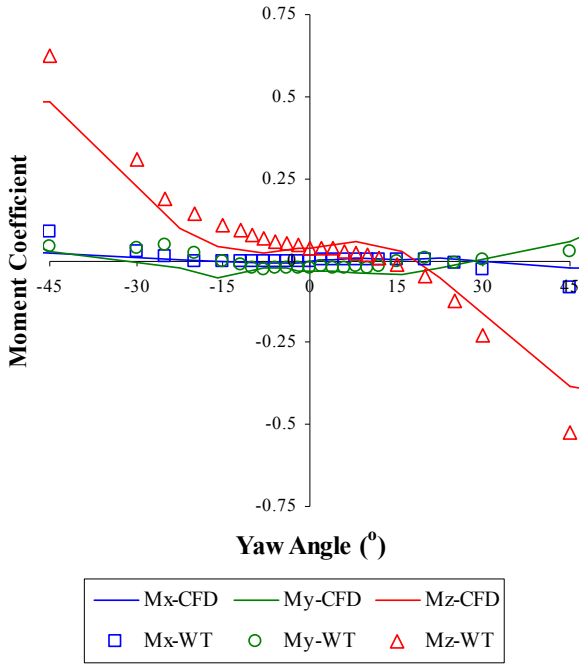

Fig. 7. Moment coefficients about the *X*, *Y* and *Z* axes against yaw angle (yaw range ±45°)

4.1.2 Flow Visualisation

Comparisons were made between the flow structures visualised in the experimental and numerical studies. This was done to

- gain an understanding of the physical phenomena that affect the fuselage aerodynamic characteristics
- qualitatively compare the numerical prediction of general flow structures with those seen during testing

An interesting flow feature observed in the numerical and experimental studies was the influence of vortices generated by the fuselage on the tail surfaces. As the yaw angle of the model is increased, a vortex is created on the leeside of the model. The development of this vortex is akin to the leading edge vortices seen on delta wings at high angles of attack. The vortex remains alongside the fuselage for yaw angles up to 45°. The location of the vortex core adjacent to the fuselage is highlighted in the Figure 6 inset. The rotation imparted on the flow can be seen in the main section of Figure 8. The numerical simulations capture these features and provide a means to better understand their effect on the tail surfaces of the model.

In Figure 9 streamlines are used to illustrate the location of the vortex generated by the fuselage. The figures show good agreement with the wind tunnel images. The location of the vortex core is similar, along with the redirection of the flow through the tail. The different flow onset angles can be seen to shift the location of the vortex slightly. Unfortunately, suitable flow visualisation was not available for a comparison of identical onset flow angles.

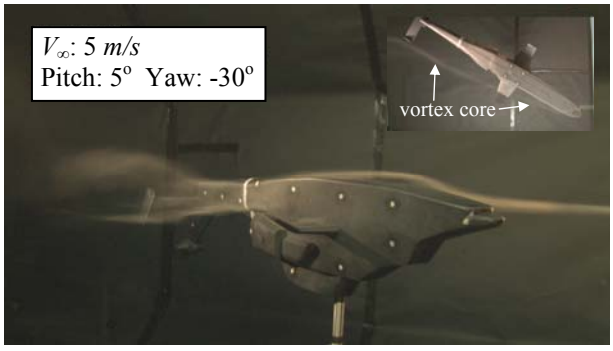

Fig. 8. Flow visualisation of vortex structure observed during wind tunnel testing (pitch: 5°, yaw: -30)

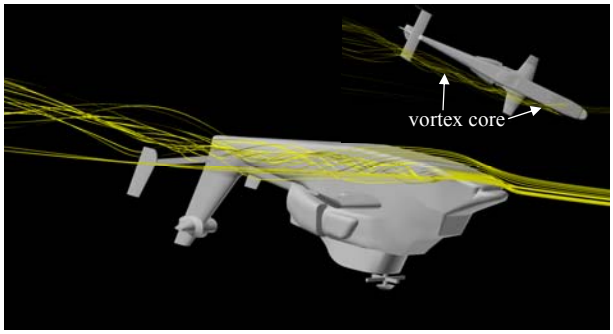

Fig. 9. Flow visualisation of vortex structure observed in numerical simulation (pitch: 0°, yaw: -22.5°)

The vector field in Figure 9 highlights the impact that the fuselage vortex has on the flow direction through the tail. At -22.5° yaw, the outer vertical fin on the leeside of the model sees a locally negative yaw angle, causing it to contribute a destabilising moment on the fuselage. This may have implications on the stability of the fuselage, particularly in the case of a fuselage being transported as a slung load. The complex interaction between the fuselage vortex and the local flow onset angle at the tail is challenging to predict, making it difficult to correctly simulate the moment contribution of the tail surfaces.

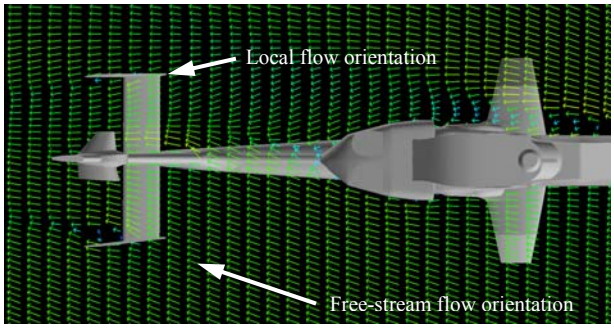

Fig. 10. Velocity vectors illustrating flow orientation through tail (pitch: 0°, yaw: -22.5°)

4.2 CFD Solver Comparison

A benchmark case was run to establish a level of confidence in *OpenFOAM* as a substitute to *Fluent*. The results for both solvers are compared in the table and figures below.

The global lift, drag and side force coefficients predicted by *OpenFOAM* and *Fluent* are listed in Table 1. The drag coefficients (C_D) compare well. The dominant pressure contribution to drag is similar for both solvers; slight differences occur for the viscous component. The lift coefficient (C_L) has the largest deviation. Compared to *Fluent, OpenFOAM* under predicts the lift by approximately 8 %. This deviation can be mainly attributed to differences in the pressure contribution. The viscous component of lift is shown to be relatively small for both solvers. The predicted side force coefficients (C_S) have similar trends to the lift coefficient. *OpenFOAM* under predicts the negative side force by approximately 5 %. Again, the pressure contribution is dominant and the viscous contribution is minimal.

		Fluent	OpenFOAM	Δ%
C_D	Pressure	1.08E-02	1.07E-02	
	Viscous	1.56E-03	1.88E-03	
	Total	**1.24E-02**	**1.25E-02**	**1.2**
C_L	Pressure	4.21E-03	3.92E-03	
	Viscous	1.06E-05	-6.04E-05	
	Total	**4.22E-03**	**3.86E-03**	**-8.3**
C_S	Pressure	-3.66E-03	-3.82E-03	
	Viscous	1.62E-05	6.85E-06	
	Total	**-3.64E-03**	**-3.81E-03**	**4.7**

Table 1. Drag, lift and side force coefficient comparison

Comparing the pressure distributions at the centreline of the fuselage gives insight into the differences between the *OpenFOAM* and *Fluent* results. The pressure coefficient (C_p) along the upper centreline is shown in Figure 11. The pressure coefficient along the lower centreline is shown in Figure 12.

The general trends predicted by the solvers compare well. Relative to *Fluent*, *OpenFOAM* predicts higher values at sharp convex regions where the pressure coefficient is negative. In areas where the pressure coefficient is positive, *OpenFOAM* generally predicts lower values. A low pressure wake affects the region behind the rotor hub. The *Fluent* results predict a lower pressure in this area than the *OpenFOAM* results. A similar trend can be seen in other research that compares *OpenFOAM* and *Fluent* simulations [1]. This suggests that the variations seen are not specific to this geometry.

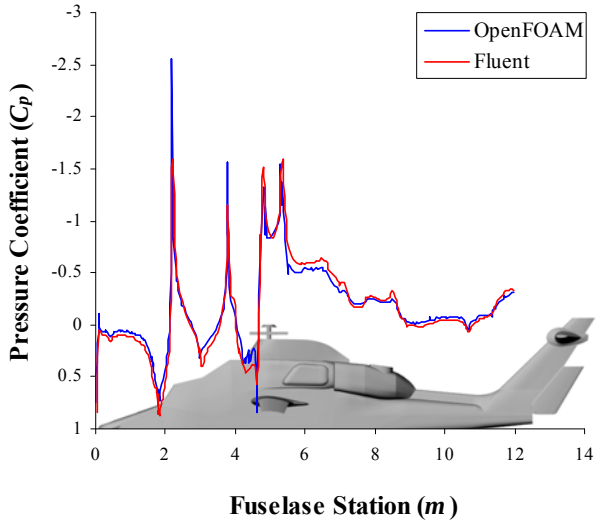

Fig. 11. Pressure coefficient distribution along the upper centreline

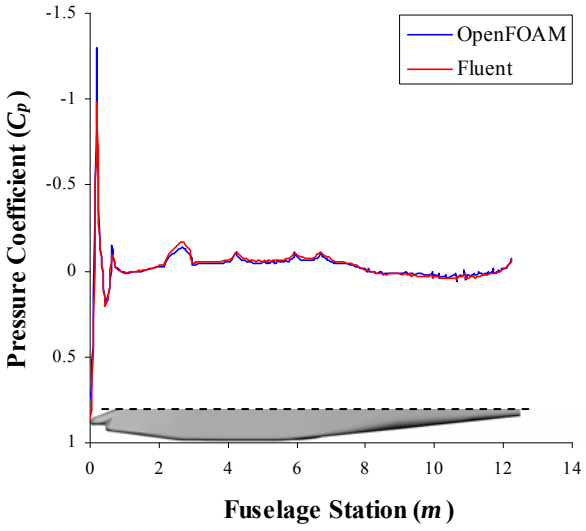

Fig. 12. Pressure coefficient distribution along the lower centreline

4.3 Wind Tunnel Support Interference

The interference caused by the wind tunnel supports was modelled using *OpenFOAM*. A range of pitch and yaw attitudes were simulated with and without the wind tunnel support. Comparisons between the numerical predictions and the wind tunnel data are shown in Figures 13 and 14.

Figure 13 shows the variation in body force coefficients for a range of pitch angles when using the rotor hub mount. The simulated force coefficients show reasonable agreement with the experimental data, particularly for pitch angles between -4° and 12°. Beyond 12° pitch there is a clear divergence between the numerical and experimental results for C_X and C_Z. The wind tunnel data indicates a sudden drop in lift and an increase in drag at approximately 15° yaw. Flow separation on the horizontal surfaces and about the fuselage is the likely cause. For angles approaching stall the wall function treatment is no longer a valid assumption and contributes to the divergence of the results.

In Figure 13, the inclusion of the wind tunnel support is seen to generally improve the correlation between the numerical and experimental results. This is particularly evident for the C_Z force coefficient. Including the support shifts the results predicted by the simulations towards the wind tunnel data. At 0° pitch the numerical results are improved by 30 % by modelling the support. Improvement in the correlation between C_Y is also evident for positive pitch angles. The C_X force coefficient is largely unchanged by modelling the support.

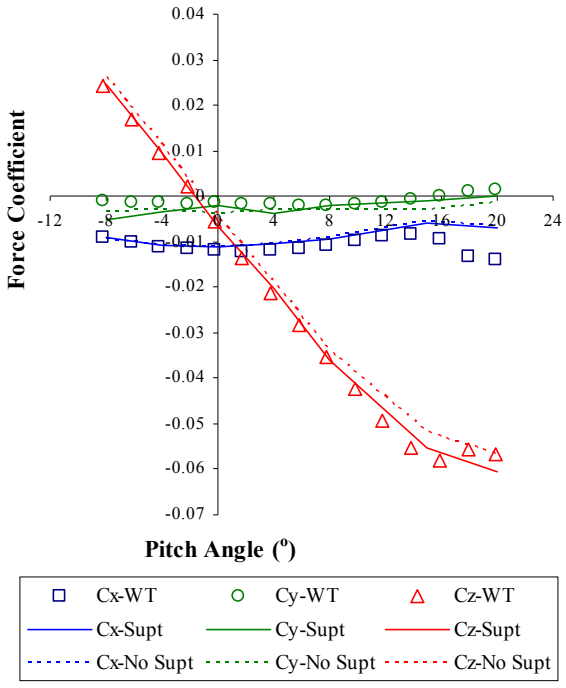

Fig. 13. Force coefficients in the *X*, *Y* and *Z* directions

An assessment of the support interference in the side mount configuration is presented in Figure 14. The variation of the force coefficients is shown for a range of yaw angles. Good agreement between the numerical and experimental results can generally be seen for the range of angles shown. An exception to this is for the C_Z force coefficient. Beyond 14° yaw the numerical and experimental results diverge. Modelling the support improves the correlation, however, discrepancies still remain. The other force coefficients, C_X and C_Y, are largely unaffected by modelling the support. The C_Y coefficient diverges from the experimental results by approximately 10 % for yaw angles above 12°. Interestingly, the wind tunnel data in Figure 14 does not indicate significant flow separation at high angles. The vortices generated by the fuselage may help to keep the flow attached at high angles. A similar behaviour has been observed in other helicopter fuselage simulations [6]. Another contributing factor is the change in flow direction through the tail due to the fuselage vortices. When combined with the yaw offset of the vertical tail fins the local yaw angle seen by the tail surfaces is significantly reduced, potentially delaying the onset of flow separation.

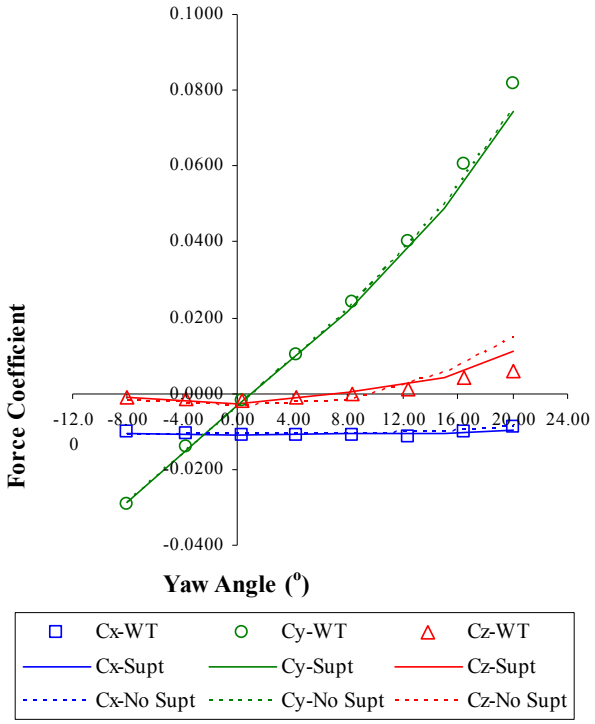

Fig. 14. Force coefficients in the *X*, *Y* and *Z* directions

5 Concluding Remarks

A database of aerodynamic coefficients has been developed to support flight dynamic and slung load modelling of an ADF helicopter fuselage. A combination of numerical and experimental techniques was utilised in the investigation.

The experimental approach involved the testing of a 1:10 scale wind tunnel model in the DSTO Low Speed Wind Tunnel. Aerodynamic force and moment data was collected for a range of onset flow angles and model configurations. Flow visualisation was conducted to provide a qualitative assessment of the flow structures that influence the fuselage aerodynamic characteristics.

The commercial CFD solver *ANSYS Fluent* was used for the preliminary numerical investigation. Predicted force coefficients were shown to compare well with the experimental results for the lower range of flow onset angles tested. At large angles, the results diverged significantly. The moment coefficients predicted showed some agreement. Comparisons were made between the flow structures observed during the wind tunnel tests and the flow structures seen in the simulations. Generally good agreement was seen. The numerical results illustrated the complex interaction between vortices generated by the fuselage and the local flow orientation through the tail surfaces. These complex flow interactions present a significant challenge to correctly modelling the force and moment contribution of the tail surfaces.

A second numerical investigation was conducted using the open source CFD solver *OpenFOAM*. To establish a level of confidence, comparisons were made between *OpenFOAM* and *Fluent* using a benchmark case. Good agreement was shown between the global force coefficients and the pressure distribution at the model centreline. *OpenFOAM* was then used to assess the interference effects of the wind tunnel supports. The CFD simulations showed an influence on the global force coefficients due to the wind tunnel supports. However, further investigation is required to better understand the differences in the results and the limitations of the modelling approach.

References

[1] Gasparella E, Ponza R, Benini E. Comparative assessment of two CFD solvers for the aerodynamic performance prediction of helicopter components. *37th European Rotorcraft Forum*, Italy, 91, 2011.

[2] Rodriguez B, Benoit C, Gardarein P. Unsteady computation of the flowfield around a helicopter rotor with model support. 3rd AIAA Aerospace Sciences Meeting and Exhibit (Reno - USA), 2005

[3] Filippone A, Michelsen J.A. Aerodynamic drag prediction of helicopter fuselage. *The Aeronautical Journal*, pp 175 – 184, 2007

[4] Patankar S.V. *Numerical Heat Transfer and Fluid Flow*, Taylor & Francis, 1980.

[5] Menter F.R. Improved two-equation k-ω turbulence models for aerodynamic flows. *NASA TM 103975*, 1992.

[6] Lehmann R, Reddy R, Armfield S. Numerical and experimental investigation of helicopter fuselage aerodynamics. *17th Australasian Fluid Mechanics Conference*, Auckland, New Zealand, December 2010.

Copyright Statement